

An orally available small molecule BCL6 inhibitor effectively suppresses diffuse large B cell lymphoma cells growth *in vitro* and *in vivo*

Yajing Xing¹, Weikai Guo¹, Min Wu¹, Jiuqing Xie¹, Dongxia Huang¹, Pan Hu¹, Miaoran Zhou², Qiansheng Zhang¹, Peili wang¹, Xin Wang¹, Guixue Wang³, Huangan Wu², Cili Zhou², Yihua Chen¹, Mingyao Liu¹, Zhengfang Yi¹, and Zhenliang Sun⁴

¹East China Normal University

²Shanghai University of Traditional Chinese Medicine

³Chongqing University

⁴Shanghai University of Medicine and Health Sciences

April 05, 2024

Abstract

Background and Purpose: The transcription factor B cell lymphoma 6 (BCL6) is an oncogenic driver of diffuse large B cell lymphoma (DLBCL). Blocking the protein-protein interactions of BCL6 and its corepressors has been proposed as an effective approach for the treatment of DLBCL. However, BCL6 inhibitors with excellent drug-like properties are rare. Hence, the development of BCL6 inhibitors is worth pursuing. **Experimental Approach:** We screened our internal chemical library by luciferase reporter assay and Homogenous Time Resolved Fluorescence (HTRF) assay and a small molecule compound named WK500B was identified. The binding affinity between WK500B and BCL6 was evaluated by surface plasmon resonance (SPR) assay and the binding mode of WK500B and BCL6 was predicted by molecular docking. The function evaluation and anti-cancer activity of WK500B was detected by immunofluorescence assay, Real-Time Quantitative PCR, cell proliferation assay, cell cycle assay, cell apoptosis assay, enzyme-linked immunosorbent assay (ELISA) and animal models. **Key Results:** WK500B engaged BCL6 inside cells, blocked BCL6 repression complexes, reactivated BCL6 target genes, killed DLBCL cells and caused apoptosis as well as cell cycle arrest. In animal models, WK500B inhibited germinal centre (GC) formation and DLBCL tumor growth without toxic and side effects. Moreover, WK500B showed favourable pharmacokinetics and presented superior druggability compared to other BCL6 inhibitors. **Conclusions and Implications:** WK500B showed strong efficacy and favourable pharmacokinetics and presented superior druggability compared to other BCL6 inhibitors. So, WK500B is a promising candidate that could be developed as an effective orally available therapeutic agent for DLBCL.

Full Title

An orally available small molecule BCL6 inhibitor effectively suppresses diffuse large B cell lymphoma cells growth *in vitro* and *in vivo*

Running Title

A BCL6 inhibitor suppresses lymphoma cells growth

Authors

Yajing Xing^{1,4,#}, Weikai Guo^{1,#}, Min Wu^{1,#}, Jiuqing Xie¹, Dongxia Huang¹, Pan Hu¹, Miaoran Zhou³, Qiansen Zhang¹, Peili Wang¹, Xin Wang¹, Guixue Wang⁴, Huangan Wu³, Cili Zhou³, Yihua Chen¹, Mingyao Liu^{1,2}, Zhengfang Yi^{1,2,*} and Zhenliang Sun^{1,2,*}

Affiliations

¹East China Normal University and Shanghai Fengxian District Central Hospital Joint Center for Translational Medicine, Shanghai University of Medicine & Health Sciences Affiliated Sixth People's Hospital South Campus, 201499, Shanghai

²East China Normal University and Shanghai Fengxian District Central Hospital Joint Center for Translational Medicine, Shanghai Key Laboratory of Regulatory Biology Institute of Biomedical Sciences and School of Life Sciences, East China Normal University, Shanghai 200241, China

³Shanghai University of Traditional Chinese Medicine, Shanghai, 201203, China

⁴Key Laboratory for Biorheological Science and Technology of Ministry of Education, State and Local Joint Engineering Laboratory for Vascular Implants, Bioengineering College of Chongqing University, Chongqing, 400030, China

Corresponding Authors

*Zhenliang Sun: Phone: +86-21-57416150. E-mail: zhenliang6@126.com

*Zhengfang Yi: Phone: +86-21-54345016. E-mail: zfyi@bio.ecnu.edu.cn

Author Contributions

Y.X., W.G. and M.W. contributed equally to this work. Y.X., W.G., X.W., H.W., C.Z., Y.C., M.L. Z.Y., and Z.S. designed the experiments. Y.X., W.G, M.W., X.J., D.H., P.H., M.Z., Q.Z., and P.W. performed the experiments. Y.X., W.G, M.W., X.J., D.H., Z.Y., M.L., G.W. and Y.C. performed the data analysis. Y.X., W.G, M.W., Z.Y., M.L. and Y.C. wrote the manuscript.

Word count: 5379

Data availability statement

The data that support the findings of this study are available from the corresponding author upon reasonable request. Some data may not be made available because of privacy or ethical restrictions.

Acknowledgements

We thank Dr. Ari Melnick (Weill Cornell Medical College, Department of Hematology/Oncology, New York, NY, USA) for support (GAL4)₅-TK-LUC and the GAL4-DBD-BCL6^{BTB} expression plasmids.

This work was supported by the grants from Major State Basic Research Development Program of China (2018YFA0507001), China Postdoctoral Science Foundation (2020M681233), National Natural Science Foundation of China (82073310, 81773204, 81973160, 81830083, 81872418), China Innovation Program of Shanghai Municipal Education Commission (2017-01-07-00-05-E00011), The Science and Technology Commission of Shanghai Municipality (20JC1417900, 21S11902000), Shenzhen Municipal Government of China (KQTD20170810160226082), ECNU Construction Fund of Innovation and Entrepreneurship Laboratory (44400-20201-532300/021), and ECNU Multifunctional Platform for innovation (011).

Conflict of interest statement

The authors declare that they have no competing interests.

Abstract

Background and Purpose: The transcription factor B cell lymphoma 6 (BCL6) is an oncogenic driver of diffuse large B cell lymphoma (DLBCL). Blocking the protein-protein interactions of BCL6 and its corepressors has been proposed as an effective approach for the treatment of DLBCL. However, BCL6 inhibitors with excellent drug-like properties are rare. Hence, the development of BCL6 inhibitors is worth pursuing.

Experimental Approach: We screened our internal chemical library by luciferase reporter assay and Homogenous Time Resolved Fluorescence (HTRF) assay and a small molecule compound named WK500B was identified. The binding affinity between WK500B and BCL6 was evaluated by surface plasmon resonance (SPR) assay and the binding mode of WK500B and BCL6 was predicted by molecular docking. The function evaluation and anti-cancer activity of WK500B was detected by immunofluorescence assay, Real-Time Quantitative PCR, cell proliferation assay, cell cycle assay, cell apoptosis assay, enzyme-linked immunosorbent assay (ELISA) and animal models.

Key Results: WK500B engaged BCL6 inside cells, blocked BCL6 repression complexes, reactivated BCL6 target genes, killed DLBCL cells and caused apoptosis as well as cell cycle arrest. In animal models, WK500B inhibited germinal centre (GC) formation and DLBCL tumor growth without toxic and side effects. Moreover, WK500B showed favourable pharmacokinetics and presented superior druggability compared to other BCL6 inhibitors.

Conclusions and Implications: WK500B showed strong efficacy and favourable pharmacokinetics and presented superior druggability compared to other BCL6 inhibitors. So, WK500B is a promising candidate that could be developed as an effective orally available therapeutic agent for DLBCL.

Keywords: BCL6, DLBCL, BTB domain, GC, small molecule inhibitor

Bullet Point Summary

What is already known:

Targeting BCL6 is an effective approach for the treatment of DLBCL.

No inhibitors that directly target BCL6 have been approved by the FDA.

What this study adds:

WK500B exhibits potent efficacy against DLBCL *in vitro* and *in vivo*.

WK500B shows favourable pharmacokinetic and presents superior druggability compared to other reported BCL6 inhibitors.

What is the clinical significance:

WK500B could be a promising therapeutic drug candidate for DLBCL.

Introduction

Diffuse large B cell lymphoma (DLBCL) which arises from the germinal centre (GC) and exhibits highly aggressive and rapid progression is the most common form of non-Hodgkin lymphoma (NHL) (Basso & Dalla-Favera, 2015; Mlynarczyk, Fontan & Melnick, 2019; Teras, DeSantis, Cerhan, Morton, Jemal & Flowers, 2016). Approximately 60%-70% of DLBCL patients can be cured by using a first-line therapy regimen that consists of the combination of a CD20 monoclonal antibody with cyclophosphamide, hydroxyrubicin, oncovin and prednisone (R-CHOP) (Coiffier & Sarkozy, 2016). Despite major advances in the treatment of DLBCL, up to 50% of the patients will relapse or become refractory to this treatment and die of their disease (Coiffier & Sarkozy, 2016; Crump et al., 2017). The development of chimeric antigen receptor (CAR)-T cell therapy may be a boon for relapsed/refractory patients, however, not all patients respond to CAR-T therapy, and only approximately 50% of those progress within 12 months (Neelapu et al., 2017). Novel therapies that improve the outcome for DLBCL remain imperative.

The BTB/POZ transcriptional repressor BCL6, is a master regulator essential for the GC reaction, which is necessary for humoral immunity and has emerged as a critical therapeutic target for DLBCL (Cerchiatti & Melnick, 2013; Leeman-Neill & Bhagat, 2018; Wagner, Ahearne & Ko Ferrigno, 2011). BCL6 contains six C₂H₂ zinc finger domain at its C-terminus, which interacts with DNA sequences (Ye et al., 1993). The N-terminal BTB-POZ domain mediates dimerization and recruits the corepressors silencing mediator of retinoid and thyroid receptor (SMRT), nuclear receptor corepressor (N-CoR) and BCL6 corepressor (B-CoR) to a

specific groove motif (Ahmad et al., 2003; Dhordain et al., 1997; Huynh, Fischle, Verdin & Bardwell, 2000), which is required for the repression of target genes involved in DNA damage responses and proliferation checkpoints (Ci et al., 2009; Phan & Dalla-Favera, 2004; Ranuncolo et al., 2007; Ranuncolo, Polo & Melnick, 2008). The middle portion, RD2, interacts with the corepressor MTA3 and represses genes involved in plasma cell differentiation (Tunyaplin, Shaffer, Angelin-Duclos, Yu, Staudt & Calame, 2004). Dysregulation of BCL6 expression associated with promoter translocations or point mutations has been shown to play a central role in DLBCLs (Leeman-Neill & Bhagat, 2018; Pasqualucci, Migliazza, Basso, Houldsworth, Chaganti & Dalla-Favera, 2003; Polo et al., 2007; Ye et al., 1993). Constitutive expression of BCL6 in mice increases the risk of the development of DLBCL, similar to that observed in human disease (Baron et al., 2004; Cattoretti et al., 2005). Delivery of shRNA to DLBCL cells, which results in the loss of BCL6 biological activity, kills DLBCL cells, indicating that BCL6 is an attractive target for DLBCL treatment (Phan & Dalla-Favera, 2004). A peptidomimetic BCL6 inhibitor RI-BPI inhibits the recruitment of BCL6^{BTB} corepressors and causes de-repression BCL6 target genes by binding to the BCL6 BTB domain (Cerchietti et al., 2009). More importantly, it can kill DLBCL cell lines and DLBCL patients cells (Cerchietti et al., 2009), demonstrating that inhibition of the BCL6^{BTB}-corepressor interaction and reactivation of BCL6 target genes are a useful therapeutic strategy for DLBCL treatment.

At present, several BCL6 small molecule inhibitors have been reported, which demonstrates the feasibility of developing BCL6 inhibitors that directly bind to the BCL6 BTB domain (Cardenas et al., 2016; Cerchietti et al., 2010; Cheng et al., 2018; Kamada et al., 2017; Kerres et al., 2017; McCoull et al., 2017; Yasui et al., 2017). However, no such inhibitor has been enrolled in a clinical-trial. For example, the compounds 79-6 and FX1 directly bind to BCL6^{BTB}, reactivate BCL6 target genes and inhibit the proliferation of DLBCL cells *in vitro* and *in vivo* (Cardenas et al., 2016; Cerchietti et al., 2010). However, the weak activities of 79-6 and FX1 and the fact that they are based on the skeleton of rhodamine may be detrimental and potential limitations for further drug development (Mendgen, Steuer & Klein, 2012; Tomasic & Peterlin Masic, 2012). Other reported small molecule inhibitors can bind to BCL6^{BTB} and disrupt the interaction between BCL6 and corepressors in a micromolar range or even a nanomolar range *in vitro*, but their effects on the biological functions of BCL6 *in vivo* have not been further studied, which may be due to their poor pharmacokinetic/pharmacodynamic properties or other reasons (Cheng et al., 2018; Kamada et al., 2017; Kerres et al., 2017; McCoull et al., 2017; Yasui et al., 2017). Therefore, there is still a long way to go in terms of screening novel BCL6 inhibitors with high druggability for DLBCL therapy.

We showed that WK500B, a novel synthetic small molecule compound, directly bound to BCL6^{BTB}, significantly inhibited the BCL6^{BTB}/SMRT interaction, reactivated BCL6 target genes in a concentration-dependent manner, killed DLBCL cell lines and caused cell cycle arrest and apoptosis. More importantly, WK500B showed favourable pharmacokinetics, resulting in the disruption of the germinal centre formation and the affinity maturation of immunoglobulins in mice at a low dose, and it strongly suppressed the growth of DLBCL *in vivo*. Furthermore, no cases of toxic effects were noted. Taken together with the fact that WK500B is more potent both *in vitro* and *in vivo*, is orally available and shows superior druggability compared with other reported BCL6 inhibitors, it seems that WK500B could be a promising therapeutic drug candidate for DLBCL.

Methods

2.1. Luciferase reporter assay

The reporter construct (GAL4)₅-TK-LUC and the GAL4-DBD-BCL6^{BTB} expression plasmid were kindly provided by Dr. Ari Melnick (Weill Cornell Medical College, Department of Haematology/Oncology, New York, NY, USA.) A TK- Renilla luciferase plasmid was included as an internal control (Promega, WA, USA). 293T cells were cotransfected with (GAL4)₅-TK-LUC and GAL4-DBD-BCL6^{BTB} or GAL4-DBD plus a TK-Renilla reporter construct using Lipofectamine 2000 (Thermo Fisher Scientific). After transfection for 6 h, the cells were treated with the compounds for 24 h. A dual luciferase assay was performed according to the manufacturer's guidelines (Promega, WA, USA).

2.2. BCL6 Protein and SMRT Peptide

The DNA segment coding for the BCL6 BTB domain (5-129) with mutations in C8Q, C67R and C84N was cloned into a vector containing a C-terminal GST tag. The construct was expressed in *E. coli* BL21 (DE3), and the culture was incubated at 18 with 0.5 mM IPTG for 18 h. BCL6^{BTB} protein was purified by glutathione agarose resin and dialyzed with PBS. The peptide SMRT (1414-1430) with a 6His tag was synthesized by Abace Biology Company.

2.3. Homogenous Time Resolved Fluorescence (HTRF) Assay

The HTRF assay in 384-well plates (Greiner Bio-one, 784045) was performed according to the manufacturer's instructions (Cisbio). Briefly, a total volume of 8 μ L of BCL6-GST protein and 6His-SMRT peptide were added to each well, and then 2 μ L of diluent buffer with the compounds to be tested was added. After 1 h, a total volume of 10 μ L of anti-6His-XL665 (Cisbio) and anti-GST-Tb (Cisbio) was added to reach a 20 μ L final volume. After overnight incubation, the plate was read on a microplate reader (BioTek Cytation5) at 665 nm and 620 nm.

2.4. Surface plasmon resonance (SPR) Assay

A Biacore T200 instrument (GE Healthcare) equipped with a CM5 sensor chip (GE Healthcare) was used to monitor binding interactions via SPR. The BCL6^{BTB} protein was immobilized on CM5 using amine-coupling at a flow rate of 10 μ L/min in 10 mM sodium acetate buffer (pH 4.0). Then, 0.1 mg/mL BCL6^{BTB} protein was injected for 420 s, and the surface was blocked by 1 M ethanolamine. The kinetics and affinity studies were performed in 25 mM HEPES, pH 7.5, 150 mM NaCl, 0.05% (v/v) Tween-20 and 5% DMSO at 25 °C. Various concentrations of compounds were injected into the flow system. Data analysis was performed using Biacore T200 Plus Evaluation Software (GE healthcare).

2.5. Cell culture and animals

Various cell lines were used including: 293T, SUDHL4, SUDHL6, OCI-Ly7, Farage, DOHH2, NCM460, PNT1A, LO2 and HAF. The cell lines SUDHL4, SUDHL6, Farage, NCM460, LO2, HAF and 293T were purchased from ATCC. OCI-Ly7 and DOHH2 were obtained from the DSMZ German collection of microorganisms and cell cultures and PNT1A was obtained from the ECACC. SUDHL4, SUDHL6, Farage, DOHH2, NCM460, PNT1A and LO2 were grown in RPMI-1640 medium (Gibco), and OCI-Ly7 was maintained in IMDM (Gibco). 293T cells were cultured in DMEM, and HAF cells were grown in DMEM with 2 mM glutamine. The medium was supplemented with 10% FBS (Gibco) and 1% penicillin-streptomycin (Gibco). All cells were incubated at 37 in a humidified atmosphere with 5% CO₂.

All animals were obtained from the Animal Centre of East China Normal University. All procedures involving animals were approved by the Animal Investigation Committee of the Institute of Biomedical Sciences, East China Normal University.

2.6. Immunofluorescence assay

SUDHL4 cells were exposed to WK500B for 24 h, fixed with 4% paraformaldehyde, permeabilized with 0.3% Triton X-100 and blocked with 1% BSA. The cells were incubated with the antibodies against BCL6 (CST, 14895) and SMRT (Invitrogen, MA1-842) overnight. Cells were then stained with secondary antibodies and DAPI was used to visualize the nuclei. Images were acquired on a confocal microscope (Leica).

2.7. Real-Time Quantitative PCR

SUDHL4 and Farage cells were treated with compounds for 24 h and lysed with TRIzol reagent (Invitrogen). RNA was extracted and reverse transcribed into cDNA with the Prime Script RT Reagent Kit (Takara). The cDNA was then used as the template for the RT-qPCR reaction and the RT-qPCR reaction was performed using SYBR-Green (Takara) on QuantStudio(r)3 Real-Time PCR System (Applied Biosystems). The sequences of primers used in the study were as follows:

p53: CCCTTCCCAGAAAACCTACC and AATCAACCCACAGCTGCAC,

CDKN1A: CTGAAGGGTCCCCAGGTG and TAGGGCTTCCTCTTGGAGAA,
CXCR4: AGGCCCTAGCTTTCTTCCAC and CTGCTCACAGAGGTGAGTGC,
CD69: CTGGTCACCCATGGAAGTG and CATGCTGCTGACCTCTGTGT,
 β -actin: TGAAGTGTGACGTGGACATC and CATACTCCTGCTTGCTGATC.

2.8. Cell Proliferation Assay

Cell viability was tested by an MTS assay (Promega, WA, USA). Cells were seeded in 96-well plates and then treated with the indicated concentrations of compounds for 72 h. Then, 20 μ L of MTS was added and incubated at 37 °C for 1-2 h. The absorbance at 490 nm was measured by a SpectraMax 190 plate reader, and the IC₅₀ value was calculated using GraphPad Prism. In the drug combination assay, the CI value was calculated by Calcsyn software.

2.9. Cell Cycle Analysis

SUDHL4 cells were treated with WK500B for 24 h. Then, the cells were harvested, washed with PBS and fixed with cold 70% ethanol at 4 °C for 12 h. Subsequently, the cells were washed twice with PBS and incubated with 50 μ g/mL propidium iodide and 10 μ g/mL RNase for 30 min in the dark at room temperature. Cells were stored at 4 °C until analysis by flow cytometry (FACS Calibur, BD Biosciences).

2.10. Cell apoptosis assay

SUDHL4 cells were treated with WK500B for 24 h. Cells were collected, washed with PBS resuspended in binding buffer and incubated with Annexin V-FITC and propidium iodide in the dark for 20 min. Samples were analysed immediately by using flow cytometry (FACS Calibur, BD Biosciences).

2.11. Immunization of mice

To induce the GC reaction, 8-week-old male C57BL/6 mice were immunized with 100 μ g of 4-hydroxy-3-nitrophenylacetyl (NP)-(Santa Cruz) coupled chicken gamma globulin (CGG) (Cedarlane). Two days later mice were randomly assigned to the indicated groups and treated daily with drugs or vehicle (0.5% methyl cellulose) by intragastric gavage for 12 days. Mice were sacrificed at the peak of the GC response. Spleens were collected for flow cytometry and histology analysis, and serum was processed for ELISA assays.

2.12. GC analysis

Cell suspensions from spleens were prepared by grinding tissue through sterile wire mesh and stained with a panel of fluorescent-conjugated antibodies including PerCP/Cy5.5 conjugated anti-B220 (Biolegend, 103236), FITC-conjugated anti-FAS (BD Pharmingen, 554257), eFluor 660-conjugated anti-GL7 (Invitrogen, 50-5902-82), PerCP/Cy5.5 conjugated anti-CD4 (Biolegend, 100434), PE-conjugated anti-CXCR5 (Biolegend, 145504), and APC-conjugated anti-PD1 (Biolegend, 109112). Samples were run on a FACS Calibur (BD), and the data were analyzed with FlowJo software (TreeStar, Portland, OR).

2.13. Immunofluorescence histology

Mouse spleens were frozen in OCT compound (Sakura), and 6 μ m-thick cryostat sections were stained with biotin-conjugated peanut agglutinin (Sigma) and IgD (BD Pharmingen) at 4 °C overnight followed by incubation with donkey anti-rat IgG(H+L)-Alexa Fluor 488 (Invitrogen) and streptavidin-Cy3 (Biolegend) for 2 h at room temperature. After washing in PBST, the slides were mounted in Prolong Gold anti-fade reagent (Molecular Probes). Images were acquired by a microscope, and ImageJ software (NIH) was used to quantify the GC areas.

2.14. ELISA

Immunoglobulin levels in serum were measured by ELISA. The titres of isotype-specific antibodies were determined for the binding of NP-specific antibodies to NP₅-BSA and NP₂₃-BSA on coated plates according

to the manufacturer’s protocol (Southern Biotech). OD values at 450 nm were measured by a plate reader (BioTek).

2.15. Xenograft tumor growth

The SUDHL4 xenograft tumour models were developed by injecting 1×10^7 cells into male SCID mice (6-8 weeks of age). The mice were grouped randomly when the volume of the tumour nodules reached 100 mm^3 and were treated by gavage injection with the indicated compounds or vehicle for 18 days, and the bodyweight and tumour dimensions were measured. The tumour volume was calculated using the following equation: tumour volume = length x width x width x 0.52. At the completion of the study, the mice were euthanized, and tumours and major organs were collected.

2.16. H&E staining and IHC

Tumours and tissue specimens were fixed and embedded in paraffin. Sections were cut from the paraffin blocks. For IHC staining, samples were carried out using the VECTASTAIN ABC kit (Vector). Anti-Ki67 (1:250; Catalogue #ab15580, Abcam) was used as the primary antibody. For H&E staining, samples were stained with haematoxylin and eosin according to standard protocols.

2.17. Statistical analysis

The results are expressed as the mean \pm SD. The significance of the difference between two groups was analysed by Student’s t test. For animal experiments, data were analysed by two-way ANOVA. All experiments were performed at least three times, except for the animal experiments. All statistical analyses were carried out using GraphPad Prism 5.0 software. The significant differences in the means were determined at the level of *P < 0.05, ** P < 0.01 and ***P < 0.001.

Results

Identification of WK500B as a novel BCL6 BTB inhibitor.

To identify novel BCL6^{BTB} inhibitors with improved activities both *in vitro* and *in vivo*, a preliminary screen was performed of a library of approximately 500 compounds using a luciferase reporter assay, which allowed us to assess BCL6-mediated transcriptional repression activity, and 2 hits were identified at a concentration of $10 \mu\text{M}$ among the investigated ones. Intriguingly, these effective compounds shared the same structural skeleton of diaminopyrimidine (Supplementary Fig. 1A). Therefore, more analogs were further synthesized and modified based on the structural of diaminopyrimidine. Subsequently, those derivatives were then subjected to secondary screen to evaluate BCL6-mediated transcriptional repression activity and the disruption of BCL6^{BTB}/SMRT complex formation by a Homogenous Time-Resolved Fluorescence (HTRF) assay (Supplementary Fig. 1A). FX1, which was previously reported as a BCL6 inhibitor (Cardenas et al., 2016), was included as the positive control. Among the investigated derivatives, 7 compounds exhibited strong repression to BCL6 in luciferase reporter assay and inhibited BCL6 and SMRT interaction in HTRF assay (Fig. 1A). WK500B was identified as the most active analogues among the investigated compounds (Fig. 1B). WK500B almost completely disrupted the transcriptional repression function of the BCL6 BTB domain at $10 \mu\text{M}$, which abrogated the repression of the (GAL4)₅-TK-LUC reporter by the GAL4-DBD-BCL6^{BTB} fusion protein, whereas FX1 had little effect on the BCL6 BTB domain at the same concentration (Fig. 1C). Consistent with its greater inhibitory activity against BCL6^{BTB} versus that of FX1, WK500B blocked the interaction of the corepressor SMRT with BCL6^{BTB} with an IC₅₀ of $1.37 \pm 0.12 \mu\text{M}$, and the IC₅₀ of FX1 was $29.78 \pm 2.45 \mu\text{M}$ (Fig. 1D). To study whether WK500B could bind to the BCL6^{BTB}, a surface plasmon resonance (SPR) assay was performed (Homola, 2003). Surprisingly, WK500B directly bound to the BCL6 BTB domain with a dissociation constant (K_D) value of $1.61 \mu\text{M}$ (Fig. 1E). In addition, we also performed a molecular docking assay to predict the binding mode of the WK500B and BCL6 BTB domain. As shown in Fig. 1F, the carbonyl oxygen of the acyl residues and the N atom of the pyridinyl on the left part of WK500B were bound to the relevant amino acid residue R24. In addition, two hydrogen bonds were formed between the N-H of the piperazine ring of WK500B and the N atom of the imidazolyl group of His14. In short, these results suggest that WK500B could bind to the BCL6 BTB domain.

WK500B disrupts BCL6 BTB/SMRT complex formation and reactivates the expression of BCL6 target genes.

The above results indicated that WK500B bound to the BCL6 BTB domain with high affinity and disrupted BCL6 BTB/SMRT complex formation in the extracellular space. To assess the impact of WK500B on the BCL6 BTB/SMRT interaction inside cells, an immunofluorescence assay was performed in SUDHL4 cells. As we predicted, the colocalization of BCL6 with SMRT was disrupted by WK500B (Fig. 2A), and endogenous BCL6 expression was not affected by WK500B (Fig. 2A, Supplementary Fig. S2A). Targeting the BCL6 BTB domain could avoid the adverse effects resulting from the complete abrogation of BCL6 functions (Huang, Hatzi & Melnick, 2013; Valls et al., 2017), and WK500B had no effect on inflammatory responses (Supplementary Fig. S2B). These findings established that WK500B bound to the BCL6 BTB domain and blocked recruitment of SMRT by BCL6.

BCL6 is a transcriptional repressor that plays a key role in GC formation and the pathogenesis of DLBCLs by repressing the expression of downstream target genes through binding with corepressors at gene promoters (Huang & Melnick, 2015; Polo et al., 2007). To determine the effect of WK500B on BCL6 transcriptional repression activity, we examined the expression of BCL6 target genes in DLBCL cell lines (SUDHL4 and Farage) that were exposed to WK500B. As shown in Fig. 2B, WK500B significantly increased the reactivation of the expression of known BCL6 target genes (p53, CDKN1A, CXCR4 and CD69) (Cardenas et al., 2016; Phan & Dalla-Favera, 2004; Ranuncolo et al., 2007; Ranuncolo, Polo & Melnick, 2008) compared with the vehicle, while the positive control compound FX1 showed little effect at the same concentration. To further explore the selectivity of WK500B, Toledo cell line, which lacks BCL6 expression was then exposed to WK500B at 10 μ M for 24 h. In contrast to SUDHL4 and Farage, WK500B had no effect on any of these genes in the BCL6-independent Toledo cell line (Figure 2C). Together, these data show that WK500B disrupts BCL6 corepressor recruitment and specifically reactivates BCL6 target genes in BCL6-dependent DLBCLs.

WK500B significantly inhibits DLBCL growth and induces cell cycle arrest and apoptosis in vitro.

Most previous studies have shown that BCL6 target genes are essential for DLBCL survival and reactivating these target genes can cause DLBCL cell lethality (Cardenas et al., 2016; Cerchietti & Melnick, 2013; Valls et al., 2017). Given that WK500B significantly reactivated BCL6 target genes (Fig. 2B), five DLBCL cell lines (SUDHL4, SUDHL6, OCI-LY7, Farage and DOHH2) were exposed to WK500B for 72 h, and the viabilities of these cells were detected through an MTS assay. As expected, WK500B effectively inhibited DLBCL proliferation at low concentrations, and the IC_{50} values of different DLBCL cell lines were equal to 1 μ M (Fig. 3A, B). In addition, four normal cell lines, including the human normal liver cell line LO2, human skin fibroblast cell line HAF, human normal colon epithelium cell line NCM460 and human prostatic cell line PNT1A, were also exposed to WK500B to further explore its selectivity toward normal cells. Excitingly, WK500B had little killing effect on the normal cells even at 10 μ M ($IC_{50} > 10 \mu$ M), indicating that WK500B selectively inhibited DLBCL proliferation with low toxicity toward normal cells (Fig. 3A, B). Moreover, WK500B had an even more significant effect on inhibiting DLBCL proliferation, and its IC_{50} values were 30-fold lower than those of FX1 (Fig. 3B). Subsequently, SUDHL4 cells with lentivirus expressing BCL6 shRNA were treated with WK500B. The results indicated that WK500B could effectively inhibit control vector cells in the investigated range of 1.25 - 10.0 μ M in a dose-dependent manner, while it showed little effect on BCL6 knockdown cells in the same concentration range, supporting the notion that WK500B inhibits DLBCL cell growth by targeting BCL6 (Fig. 3C).

BCL6 mediates the survival and cell cycle progression of B-cell lymphoma cells (Polo et al., 2004). We determined whether WK500B affected DLBCL cell cycle progression and cell apoptosis by using flow cytometry. The results (Fig. 3D, E) indicated that WK500B induced significant cell cycle arrest at the S phase and caused the dose-dependent induction of apoptosis at doses of 2.5, 5.0 and 10 μ M. The positive control FX1 did not induce apoptosis or cell cycle arrest at the same concentration (data not shown). Taken together, these results demonstrated that WK500B induced the death of DLBCLs *in vitro*.

WK500B exhibits favourable pharmacokinetics and abrogates germinal centre formation in vivo.

To determine whether WK500B could serve as the prototype of BCL6 inhibitor for further clinical development, a human liver microsome study was primarily carried out to evaluate *in vitro* metabolism of WK500B. Intriguingly, WK500B had good metabolic stability *in vitro* (Supplementary Table 1). Encouraged by this result, pharmacokinetic analyses were subsequently performed after oral administration (p.o., 10 mg/kg) and intravenous injection (i.p., 5.0 mg/kg) of WK500B in mice to further gain insights into the preclinical pharmacokinetics. As shown in Supplementary Table 2, the plasma half-life ($T_{1/2}$) values were 7.93 ± 0.81 h for p.o. administration and 6.41 ± 0.87 h for i.p. injection, respectively, and relatively low plasma clearance (CL) was observed, which indicated that WK500B has improved metabolic stability *in vivo*. The mean values of the apparent volume of distribution (V_d) were very high for both p.o. and i.p. administration, which suggested that WK500B was widely distributed in tissues. In addition, the area under the curve ($AUC_{0-[\?]}$) was high for both p.o. and i.p. administration, indicating that WK500B was absorbed easily. Moreover, WK500B has excellent oral bioavailability ($F = 82.49\%$). These results demonstrated that WK500B is a bioavailable candidate for oral administration and has improved drug-likeness.

BCL6 is important for the formation of GCs for humoral immunity, and mice engineered with a mutation of BCL6 BTB have normal B cell development but fail to form GCs and show disruption of the affinity maturation of immunoglobulins (Huang, Hatzi & Melnick, 2013). To examine the impact of WK500B on GCs, C57/BL6 mice were immunized with NP₁₈CGG and treated by gavage with daily doses of WK500B and FX1 (positive control) at 50 mg/kg two days later. After 12 days of dosing, the mice were sacrificed. As expected, the WK500B treatment group showed significantly abolished GC formation (GL7⁺FAS⁺B220⁺) compared with the vehicle group (Fig. 4A). Moreover, the WK500B treatment group exhibited better inhibitory activity, with a frequency of B cells of 0.4%, than the FX1 group, in which the frequency of GC B cells was 0.9% (Fig. 4A). In addition, spleens were also subjected to immunofluorescent staining to assess the number of GCs. Ig D staining revealed normal B cell follicular structures, and staining with peanut agglutinin, a GC B cell-specific marker, showed a profound loss of GCs (Fig. 4B), similar to the results of Flow cytometric. Notably, WK500B had a more significant GC inhibitory effect than FX1.

Follicular helper T (Tfh) cells contribute to the development of GC B cells, and BCL6 also acts a pivotal part in Tfh cells (Huang, Hatzi & Melnick, 2013; Kitano et al., 2011). In mice with BCL6^{BTB} mutations, the frequency of Tfh cells was depleted compared with that in BCL6^{+/+} mice (Huang, Hatzi & Melnick, 2013). Similar to that observed in mice with conditional deletion of BCL6 in GC B cells, the proportion of Tfh cells (CXCR5⁺PD1⁺CD4⁺) was much lower in the WK500B treatment group than that in the untreated group (Fig. 4C).

Impaired immunoglobulin affinity maturation is found in mice with BCL6 BTB mutations (Huang, Hatzi & Melnick, 2013), and we next examined whether WK500B can recapitulate this phenotype by enzyme-linked immunosorbent assay (ELISA). As expected, WK500B treatment group brought about antibody-deficient mice whose titres of high-affinity immunoglobulin G1 specific to NP5-BSA as well as the total IgG1 specific to NP23-BSA were dramatically lower than the blank control group (Fig. 4D). Collectively, these results demonstrated that WK500B could effectively inhibit BCL6 biological functions *in vivo*.

WK500B effectively suppresses the growth of lymphoma without toxic effects in vivo.

To further evaluate whether WK500B could protect against DLBCL proliferation *in vivo*, SCID mouse xenograft models were established by subcutaneous injection of SUDHL4 DLBCL cells. When visible tumours reached approximately 100 mm³ in size, mice were injected with 12.5 mg/kg/day and 25 mg/kg/day WK500B or 25 mg/kg/day FX1 (positive control) or vehicle by oral administration. The tumour volume and mouse body weight were detected every three days. As expected, WK500B significantly inhibited tumour growth and had a more potent tumour-inhibitory effect than FX1 (Fig. 5A, B and C). Importantly, the expression of BCL6 target genes in tumours was more strongly reactivated in the WK500B-treated groups than in the control group, which was consistent with the *in vitro* observations (Fig. 2B), providing pharmacodynamic evidence of WK500B engaging with BCL6 in tumour tissue (Fig. 5E). In addition, the tumour tissues were analysed by immunohistochemistry (IHC). Compared with control group, the proliferation marker Ki67 was dramatically decreased in the WK500B-treated groups, which confirmed the anticancer effects of WK500B *in*

in vivo (Fig. 5F). Furthermore, we tested whether WK500B bring about toxic effects in mice. No obvious toxicity was observed according to the measurement of the mouse body weight (Fig. 5D), and the mice had no abnormal behaviour or side effects during the treatment period. Moreover, no obvious organ damage was observed based on H&E staining (Supplementary Fig. 3). To further evaluate the toxicity of WK500B in mice, C57BL/6 mice received WK500B orally at 50 mg/kg/day for 14 days, and the biochemical parameters and complete blood counts from C57BL/6 mice were examined. Intriguingly, WK500B had negligible effects on mice treated with compound (Supplementary Tables 3 and 4). Hence, these data demonstrated that WK500B is an effective anti-lymphoma agent *in vivo* and is nontoxic to animals.

WK500B synergizes with EZH2 and PRMT5 inhibitors.

Since lymphomas are typically highly heterogeneous, BCL6 inhibitors in combination with other targeted agents are required. BCL6 has been found to cooperate with EZH2 and PRMT5 to mediate GC formation (Beguelin et al., 2016; Lu et al., 2018). Then, to evaluate whether WK500B has synergistic effects with EZH2 inhibitor or PRMT5 inhibitor, we exposed SUDHL4 cells to a combination of the PRMT5 inhibitor GSK591 or the EZH2 inhibitor GSK343 with WK500B, and we observed increased de-repression of BCL6 target genes compared to that induced by either compound alone (Fig. 6A). Next, the combinatorial activity was determined by administering increasing doses of WK500B with GSK591 or GSK343 and measuring cell viability. As expected, the combination of GSK591 with WK500B more significantly suppressed DLBCL cell growth than either GSK591 or WK500B alone, resulting in a synergistic combination effect (Fig. 6B). Consistent with the findings for GSK591, synergistic killing activity in SUDHL4 cells was also observed when combining GSK343 with WK500B (Fig. 6B). Collectively, the results indicate that WK500B synergizes with the EZH2 and PRMT5 inhibitors.

Discussion

B cells transiting the GC reaction manifest many hallmarks of cancer cells, and the deregulation of BCL6 expression leads to B cell malignant transformation. BCL6 has been documented a convincing therapeutic target in DLBCL and other GC-derived lymphomas (Leeman-Neill & Bhagat, 2018). Inhibitors that disrupt interactions between BCL6^{BTB} and its corepressors show anticancer activity and lack toxicity (Cerchiotti et al., 2009; Polo et al., 2004). Although a series of BCL6 inhibitors have been reported (Fig. 7A), the IC₅₀ values of BCL6 inhibitors are high and molecules with a higher affinity for BCL6 have not been studied *in vivo* (Fig. 7B), which is perhaps due to their poor pharmacokinetic properties or other reasons (Kamada et al., 2017; Kerres et al., 2017; McCoull et al., 2017). Hence, the development of clinical-grade BCL6 inhibitors with improved drug-likeness is an urgent mission.

Here, we conducted a screen by using a luciferase reporter assay and an HTRF assay to identify a novel potent BCL6 inhibitor, WK500B, which directly bound to BCL6^{BTB}, significantly reactivated the expression of BCL6 target genes, impacted the growth of DLBCLs *in vitro* and induced apoptosis and cell cycle arrest. BCL6^{BTB} mutant mice had an impaired GC response after immunization with a T cell-dependent antigen (Huang, Hatzi & Melnick, 2013). WK500B disturbed the biological functions of BCL6 and phenocopied the BCL6^{BTB} phenotype *in vivo*, which significantly inhibited GC formation, reduced the proportion of Tfh cells and impaired immunoglobulin affinity maturation. Moreover, WK500B suppressed the growth of DLBCL cells free of eliciting detectable off-target effects against normal tissues. No inhibitors that directly target BCL6 have been approved by the FDA, which may be due to their poor pharmacokinetic/pharmacodynamic properties (Cheng et al., 2018; Kamada et al., 2017; Kerres et al., 2017; McCoull et al., 2017; Yasui et al., 2017). WK500B displayed favourable pharmacokinetics with a long plasma half-life ($T_{1/2}$) and low plasma clearance (CL) as well as a high apparent volume of distribution (V_d) and area under the curve (AUC_{0-24}). Extraordinarily, WK500B also has excellent oral bioavailability, which is not possessed by other BCL6 inhibitors. Taken together, WK500B is orally available and shows superior druggability compared with other reported BCL6 inhibitors (Fig. 7A, B).

In addition, other aspects of the BCL6 mechanism have been harnessed to design combined targeted therapy regimens (Cardenas, Oswald, Yu, Xue, MacKerell & Melnick, 2017). Combinations of WK500B with an

EZH2 inhibitor and a PRMT5 inhibitor showed enhanced anti-lymphoma activity and synergistic effects on the de-repression of BCL6 target genes. Future clinical trials will be important to investigate the efficacy of targeting BCL6 in combination with other therapies. Recent reports have implicated BCL6 as an important therapeutic target in solid tumours, including glioblastoma (Xu et al., 2017), breast cancer (Walker et al., 2015), ovarian cancer (Wang, Xu, Weng, Wei, Yang & Du, 2015) and non-small cell lung cancer (NSCLC) (Deb et al., 2017). Moreover, an increasing number of studies have shown that targeting the BCL6 BTB domain can overcome drug tolerance in cancer cells, (Duy et al., 2011; Fernando et al., 2019; Madapura et al., 2017; Song et al., 2018; Wu, Lv, Wang, Li & Guo, 2018). We conjectured that WK500B may kills other cancer cells and overcome drug tolerance, which need more experiments to verify our hypothesis. This is of great significance to expand the scope of BCL6 inhibitors.

In summary, WK500B not only disrupted BCL6 biological functions *in vitro* and *in vivo* but also presented superior druggability, and combination therapy with WK500B and other targeted chemotherapeutic agents yielded dramatic antitumour effects. Therefore, WK500B could potentially be used as a novel effective and orally available anticancer agent for treatment of DLBCL.

References

- Ahmad KF, Melnick A, Lax S, Bouchard D, Liu J, Kiang CL, *et al.*(2003). Mechanism of SMRT corepressor recruitment by the BCL6 BTB domain. *Mol Cell* 12: 1551-1564.
- Baron BW, Anastasi J, Montag A, Huo D, Baron RM, Karrison T, *et al.* (2004). The human BCL6 transgene promotes the development of lymphomas in the mouse. *Proc Natl Acad Sci U S A* 101:14198-14203.
- Basso K, & Dalla-Favera R (2015). Germinal centres and B cell lymphomagenesis. *Nat Rev Immunol* 15: 172-184.
- Beguelin W, Teater M, Gearhart MD, Calvo Fernandez MT, Goldstein RL, Cardenas MG, *et al.* (2016). EZH2 and BCL6 Cooperate to Assemble CBX8-BCOR Complex to Repress Bivalent Promoters, Mediate Germinal Center Formation and Lymphomagenesis. *Cancer Cell* 30: 197-213.
- Cardenas MG, Oswald E, Yu W, Xue F, MacKerell AD, Jr., & Melnick AM (2017). The Expanding Role of the BCL6 Oncoprotein as a Cancer Therapeutic Target. *Clin Cancer Res* 23: 885-893.
- Cardenas MG, Yu W, Beguelin W, Teater MR, Geng H, Goldstein RL, *et al.* (2016). Rationally designed BCL6 inhibitors target activated B cell diffuse large B cell lymphoma. *J Clin Invest* 126: 3351-3362.
- Cattoretti G, Pasqualucci L, Ballon G, Tam W, Nandula SV, Shen Q, *et al.* (2005). Deregulated BCL6 expression recapitulates the pathogenesis of human diffuse large B cell lymphomas in mice. *Cancer Cell* 7: 445-455.
- Cerchietti L, & Melnick A (2013). Targeting BCL6 in diffuse large B-cell lymphoma: what does this mean for the future treatment? *Expert Rev Hematol* 6: 343-345.
- Cerchietti LC, Ghetu AF, Zhu X, Da Silva GF, Zhong S, Matthews M, *et al.* (2010). A small-molecule inhibitor of BCL6 kills DLBCL cells in vitro and in vivo. *Cancer Cell* 17: 400-411.
- Cerchietti LC, Yang SN, Shaknovich R, Hatzi K, Polo JM, Chadburn A, *et al.* (2009). A peptomimetic inhibitor of BCL6 with potent antilymphoma effects in vitro and in vivo. *Blood* 113:3397-3405.
- Cheng H, Linhares BM, Yu W, Cardenas MG, Ai Y, Jiang W, *et al.*(2018). Identification of Thiourea-Based Inhibitors of the B-Cell Lymphoma 6 BTB Domain via NMR-Based Fragment Screening and Computer-Aided Drug Design. *J Med Chem* 61: 7573-7588.
- Ci W, Polo JM, Cerchietti L, Shaknovich R, Wang L, Yang SN, *et al.* (2009). The BCL6 transcriptional program features repression of multiple oncogenes in primary B cells and is deregulated in DLBCL. *Blood* 113: 5536-5548.

- Coiffier B, & Sarkozy C (2016). Diffuse large B-cell lymphoma: R-CHOP failure-what to do? *Hematology Am Soc Hematol Educ Program* 2016: 366-378.
- Crump M, Neelapu SS, Farooq U, Van Den Neste E, Kuruvilla J, Westin J, *et al.* (2017). Outcomes in refractory diffuse large B-cell lymphoma: results from the international SCHOLAR-1 study. *Blood* 130: 1800-1808.
- Deb D, Rajaram S, Larsen JE, Dospoy PD, Marullo R, Li LS, *et al.*(2017). Combination Therapy Targeting BCL6 and Phospho-STAT3 Defeats Intratumor Heterogeneity in a Subset of Non-Small Cell Lung Cancers. *Cancer Res* 77: 3070-3081.
- Dhordain P, Albagli O, Lin RJ, Ansieau S, Quief S, Leutz A, *et al.* (1997). Corepressor SMRT binds the BTB/POZ repressing domain of the LAZ3/BCL6 oncoprotein. *Proc Natl Acad Sci U S A* 94:10762-10767.
- Duy C, Hurtz C, Shojaee S, Cerchietti L, Geng H, Swaminathan S, *et al.* (2011). BCL6 enables Ph+ acute lymphoblastic leukaemia cells to survive BCR-ABL1 kinase inhibition. *Nature* 473: 384-388.
- Fernando TM, Marullo R, Pera Gresely B, Phillip JM, Yang SN, Lundell-Smith G, *et al.* (2019). BCL6 Evolved to Enable Stress Tolerance in Vertebrates and Is Broadly Required by Cancer Cells to Adapt to Stress. *Cancer Discov* 9: 662-679.
- Homola J (2003). Present and future of surface plasmon resonance biosensors. *Anal Bioanal Chem* 377: 528-539.
- Huang C, Hatzi K, & Melnick A (2013). Lineage-specific functions of Bcl-6 in immunity and inflammation are mediated by distinct biochemical mechanisms. *Nat Immunol* 14: 380-388.
- Huang C, & Melnick A (2015). Mechanisms of action of BCL6 during germinal center B cell development. *Sci China Life Sci* 58:1226-1232.
- Huynh KD, Fischle W, Verdin E, & Bardwell VJ (2000). BCoR, a novel corepressor involved in BCL-6 repression. *Genes Dev* 14:1810-1823.
- Kamada Y, Sakai N, Sogabe S, Ida K, Oki H, Sakamoto K, *et al.*(2017). Discovery of a B-Cell Lymphoma 6 Protein-Protein Interaction Inhibitor by a Biophysics-Driven Fragment-Based Approach. *J Med Chem* 60: 4358-4368.
- Kerres N, Steurer S, Schlager S, Bader G, Berger H, Caligiuri M, *et al.* (2017). Chemically Induced Degradation of the Oncogenic Transcription Factor BCL6. *Cell Rep* 20: 2860-2875.
- Kitano M, Moriyama S, Ando Y, Hikida M, Mori Y, Kurosaki T, *et al.* (2011). Bcl6 protein expression shapes pre-germinal center B cell dynamics and follicular helper T cell heterogeneity. *Immunity* 34: 961-972.
- Leeman-Neill RJ, & Bhagat G (2018). BCL6 as a therapeutic target for lymphoma. *Expert Opin Ther Targets* 22: 143-152.
- Lu X, Fernando TM, Lossos C, Yusufova N, Liu F, Fontan L, *et al.*(2018). PRMT5 interacts with the BCL6 oncoprotein and is required for germinal center formation and lymphoma cell survival. *Blood* 132: 2026-2039.
- Madapura HS, Nagy N, Ujvari D, Kallas T, Krohnke MCL, Amu S, *et al.* (2017). Interferon gamma is a STAT1-dependent direct inducer of BCL6 expression in imatinib-treated chronic myeloid leukemia cells. *Oncogene* 36: 4619-4628.
- McCoull W, Abrams RD, Anderson E, Blades K, Barton P, Box M, *et al.* (2017). Discovery of Pyrazolo[1,5-*a*]pyrimidine B-Cell Lymphoma 6 (BCL6) Binders and Optimization to High Affinity Macrocyclic Inhibitors. *J Med Chem* 60: 4386-4402.
- Mendgen T, Steuer C, & Klein CD (2012). Privileged scaffolds or promiscuous binders: a comparative study on rhodanines and related heterocycles in medicinal chemistry. *J Med Chem* 55: 743-753.

- Mlynarczyk C, Fontan L, & Melnick A (2019). Germinal center-derived lymphomas: The darkest side of humoral immunity. *Immunol Rev* 288: 214-239.
- Neelapu SS, Locke FL, Bartlett NL, Lekakis LJ, Miklos DB, Jacobson CA, *et al.* (2017). Axicabtagene Ciloleucel CAR T-Cell Therapy in Refractory Large B-Cell Lymphoma. *N Engl J Med* 377: 2531-2544.
- Pasqualucci L, Migliazza A, Basso K, Houldsworth J, Chaganti RS, & Dalla-Favera R (2003). Mutations of the BCL6 proto-oncogene disrupt its negative autoregulation in diffuse large B-cell lymphoma. *Blood* 101: 2914-2923.
- Phan RT, & Dalla-Favera R (2004). The BCL6 proto-oncogene suppresses p53 expression in germinal-centre B cells. *Nature* 432: 635-639.
- Polo JM, Dell'Oso T, Ranuncolo SM, Cerchietti L, Beck D, Da Silva GF, *et al.* (2004). Specific peptide interference reveals BCL6 transcriptional and oncogenic mechanisms in B-cell lymphoma cells. *Nat Med* 10: 1329-1335.
- Polo JM, Juszczynski P, Monti S, Cerchietti L, Ye K, Grealley JM, *et al.* (2007). Transcriptional signature with differential expression of BCL6 target genes accurately identifies BCL6-dependent diffuse large B cell lymphomas. *Proc Natl Acad Sci U S A* 104: 3207-3212.
- Ranuncolo SM, Polo JM, Dierov J, Singer M, Kuo T, Grealley J, *et al.* (2007). Bcl-6 mediates the germinal center B cell phenotype and lymphomagenesis through transcriptional repression of the DNA-damage sensor ATR. *Nat Immunol* 8: 705-714.
- Ranuncolo SM, Polo JM, & Melnick A (2008). BCL6 represses CHEK1 and suppresses DNA damage pathways in normal and malignant B-cells. *Blood Cells Mol Dis* 41: 95-99.
- Song W, Wang Z, Kan P, Ma Z, Wang Y, Wu Q, *et al.* (2018). Knockdown of BCL6 Inhibited Malignant Phenotype and Enhanced Sensitivity of Glioblastoma Cells to TMZ through AKT Pathway. *Biomed Res Int* 2018: 6953506.
- Teras LR, DeSantis CE, Cerhan JR, Morton LM, Jemal A, & Flowers CR (2016). 2016 US lymphoid malignancy statistics by World Health Organization subtypes. *CA Cancer J Clin* 66: 443-459.
- Tomasic T, & Peterlin Masic L (2012). Rhodanine as a scaffold in drug discovery: a critical review of its biological activities and mechanisms of target modulation. *Expert Opin Drug Discov* 7: 549-560.
- Tunyaplin C, Shaffer AL, Angelin-Duclos CD, Yu X, Staudt LM, & Calame KL (2004). Direct repression of prdm1 by Bcl-6 inhibits plasmacytic differentiation. *J Immunol* 173: 1158-1165.
- Valls E, Lobry C, Geng H, Wang L, Cardenas M, Rivas M, *et al.* (2017). BCL6 Antagonizes NOTCH2 to Maintain Survival of Human Follicular Lymphoma Cells. *Cancer Discov* 7: 506-521.
- Wagner SD, Ahearne M, & Ko Ferrigno P (2011). The role of BCL6 in lymphomas and routes to therapy. *Br J Haematol* 152: 3-12.
- Walker SR, Liu S, Xiang M, Nicolais M, Hatzi K, Giannopoulou E, *et al.* (2015). The transcriptional modulator BCL6 as a molecular target for breast cancer therapy. *Oncogene* 34: 1073-1082.
- Wang YQ, Xu MD, Weng WW, Wei P, Yang YS, & Du X (2015). BCL6 is a negative prognostic factor and exhibits pro-oncogenic activity in ovarian cancer. *Am J Cancer Res* 5: 255-266.
- Wu HB, Lv WF, Wang YX, Li YY, & Guo W (2018). BCL6 promotes the methotrexate-resistance by upregulating ZEB1 expression in children with acute B lymphocytic leukemia. *Eur Rev Med Pharmacol Sci* 22:5240-5247.
- Xu L, Chen Y, Dutra-Clarke M, Mayakonda A, Hazawa M, Savinoff SE, *et al.* (2017). BCL6 promotes glioma and serves as a therapeutic target. *Proc Natl Acad Sci U S A* 114: 3981-3986.

Yasui T, Yamamoto T, Sakai N, Asano K, Takai T, Yoshitomi Y, *et al.* (2017). Discovery of a novel B-cell lymphoma 6 (BCL6)-corepressor interaction inhibitor by utilizing structure-based drug design. *Bioorg Med Chem* 25: 4876-4886.

Ye BH, Lista F, Lo Coco F, Knowles DM, Offit K, Chaganti RS, *et al.* (1993). Alterations of a zinc finger-encoding gene, BCL-6, in diffuse large-cell lymphoma. *Science* 262: 747-750.

Figure legends

Fig. 1 WK500B is identified as a BCL6^{BTB}inhibitor. (A) The repression to BCL6 activity versus inhibition of interaction between BCL6 and SMRT of FX1 and 7 derivative analogs. (B) Chemical structure of WK500B. (C) WK500B attenuated BCL6^{BTB}-mediated transcriptional repression in luciferase reporter assays. (D) WK500B was tested by a HTRF assay for inhibition of the BCL6-SMRT interaction. (E) K_D of WK500B binding to BCL6 protein determined by an SPR assay. (F) The binding model of WK500B with BTB of BCL6. (*, $P < 0.05$; **, $P < 0.01$ versus control)

Fig. 2 WK500B blocks BCL6^{BTB}-mediated corepressor recruitment and induces de-repression of BCL6 target genes.(A) The colocalization of BCL6 and SMRT was disrupted by WK500B. Scale bar, 10 μm . (B) WK500B reactivated the de-repression of BCL6 target genes. (*, $P < 0.05$; **, $P < 0.01$; ***, $P < 0.001$ versus control). (C) mRNA abundance of the BCL6 target genes was measured in SUDHL4, Farage (both BCL6 dependent) and Toledo (BCL6 independent) cell lines exposed to WK500B.

Fig. 3 WK500B inhibits DLBCL cell growth and induces apoptosis *in vitro*. (A) Anti-proliferative effects of WK500B on DLBCL cell lines and normal cell lines after 72 h of treatment. (B) IC_{50} values of WK500B and FX1 in DLBCL cell lines and normal cell lines after 72 h of treatment. (C) SUDHL4 cells were transfected with BCL6 specific shRNA (shBCL6) or Scramble shRNA (shScr) and then seeded in 96-well plates and treated with WK500B. After 72 h, cell growth was measured by MTS assay. (*, $P < 0.05$; **, $P < 0.01$; ***, $P < 0.001$ versus control). (D) Cell cycle profile of SUDHL4 cells treated with WK500B for 24 h. (E) The effect on apoptosis of SUDHL4 cells that were treated with WK500B for 24 h.

Fig. 4 WK500B inhibits GC formation *in vivo*. C57BL/6 mice were immunized intraperitoneally with NP-CGG and by gavage with WK500B at a dosage of 50 mg/kg/d for 12 days. (A) Representative flow cytometry plot of splenic GC B cells (B220⁺GL7⁺FAS⁺) (left) and quantification (right). (B) Immunofluorescence histology of spleens stained for peanut agglutinin (red) and Ig D (green). Scale bars represent 100 μm . Quantification of the area of GCs was performed by ImageJ software. (C) Flow cytometry detection of Tfh cells (CD4⁺CXCR5⁺PD1⁺) (left) and quantification (right). (D) Titres of the NP-specific immunoglobulin G1 in serum measured with NP5-BSA and NP23-BSA and presented in relative units (RU) as serial dilutions of serum relative to the antibody end-point titres. (*, $P < 0.05$; **, $P < 0.01$; ***, $P < 0.001$ versus control).

Fig. 5 WK500B suppresses BCL6-driven DLBCL growth *in vivo*. SUDHL4 cells were injected subcutaneously into SCID mice. After 18 days of treatment, the mice were sacrificed, and the tumours were photographed (A) and weighed (B). Scale bars, 1 cm. Tumour volumes (C) and body weights (D) of mice treated with different compounds were measured every 3 days. (E) mRNA expression of the BCL6 target genes from tumours was measured by RT-qPCR assays. (F) Images of IHC staining of Ki67 are shown. Scale bars, 50 μm . (*, $P < 0.05$; **, $P < 0.01$; ***, $P < 0.001$ versus control).

Fig. 6 WK500B synergizes with EZH2 and PRMT5 inhibitors. (A) mRNA abundances of BCL6 target genes in SUDHL4 cells treated with 2 μM GSK591 or GSK343 for 72 h, 2 μM WK500B for 24 h, or a combination. (B) WK500B and PRMT5 inhibitor or EZH2 inhibitor cooperate to kill SUDHL4 cells, and the combination indexes (CIs) are shown at the indicated concentrations. (*, $P < 0.05$; **, $P < 0.01$; ***, $P < 0.001$ versus control).

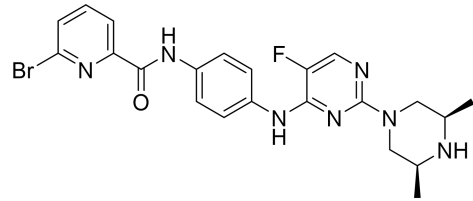
Fig. 7 Comparison of reported small molecular BCL6 inhibitors and WK500B. (A) Chemical structures of reported small molecular BCL6 inhibitors and WK500B. (B) Comparison of reported small molecular BCL6 inhibitors and WK500B. Y, indicates that the title requirement is met. N, indicates that

the datum was not reported. Otherwise, the violation is listed in detail. cLogP and tPSA were calculated using Chemdraw.

A

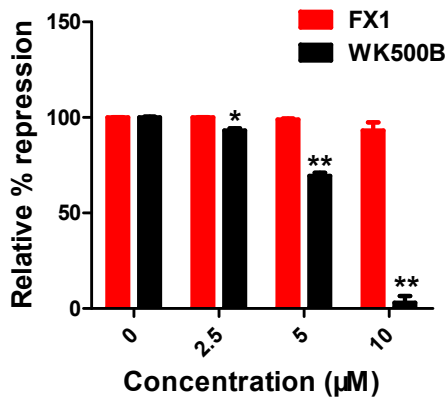
Compound	Relative repression to BCL6 (at 10 μ M)	HTRF IC ₅₀ (μ M)
FX1	3.82%	37.68
WK507B	59.57%	4.85
WK512A	57.46%	6.03
WK500B	95.69%	1.39
WK530B	83.03%	3.44
WK519B	43.80%	5.08
WK521B	48.07%	3.50
WK535E	28.60%	9.64

B

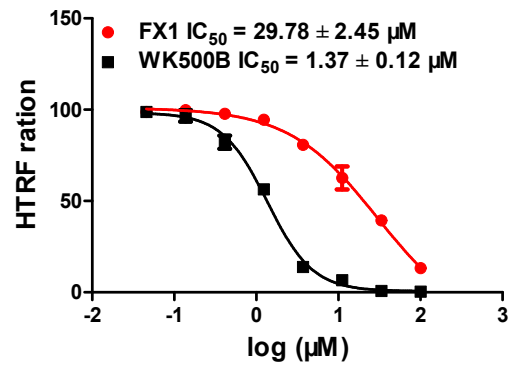


Chemical Formula: C₂₂H₂₃BrFN₇O
Molecular Weight: 500.38
WK500B

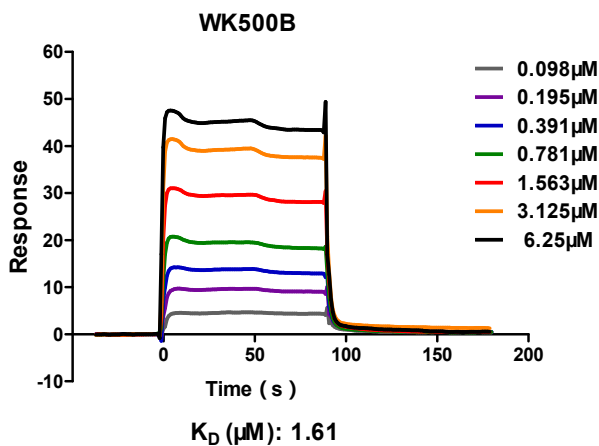
C



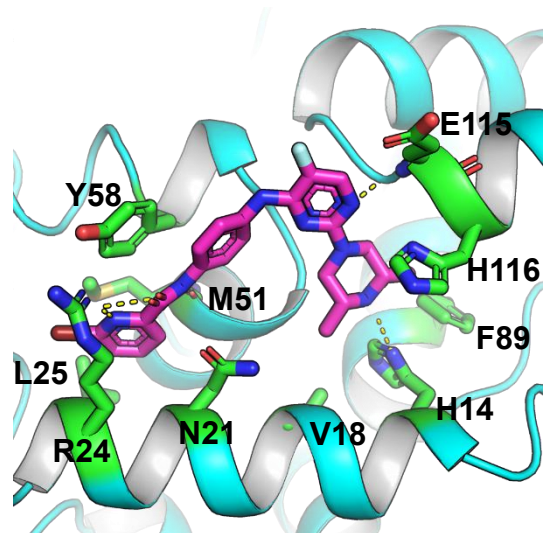
D

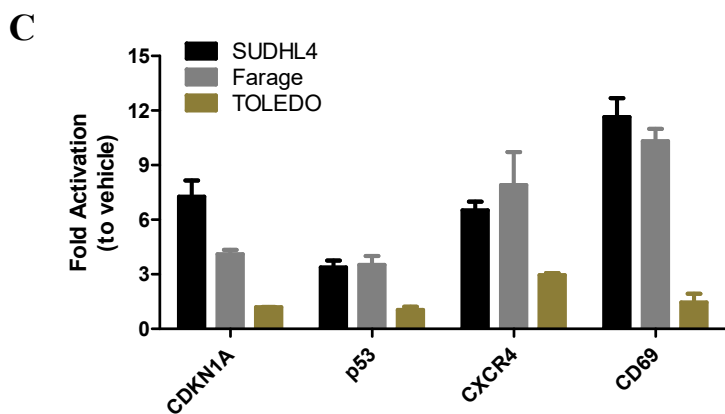
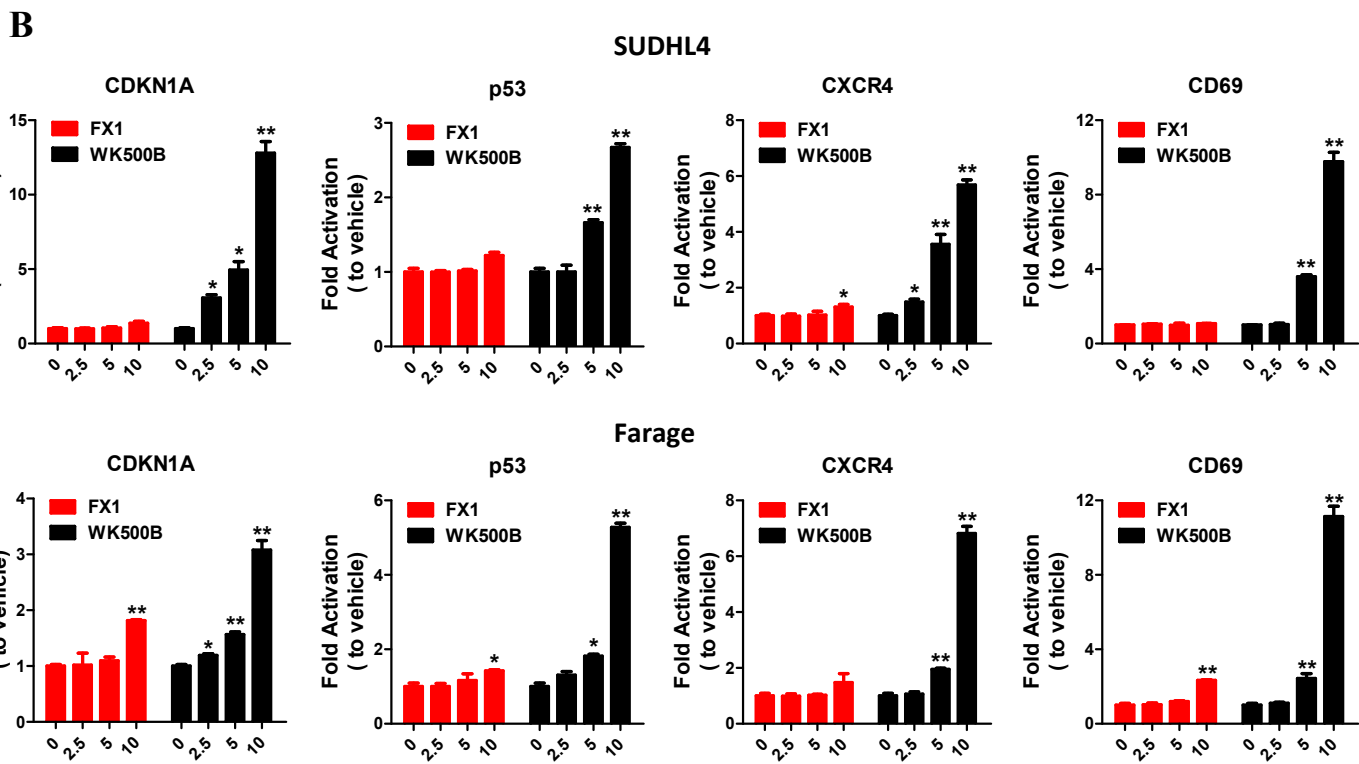
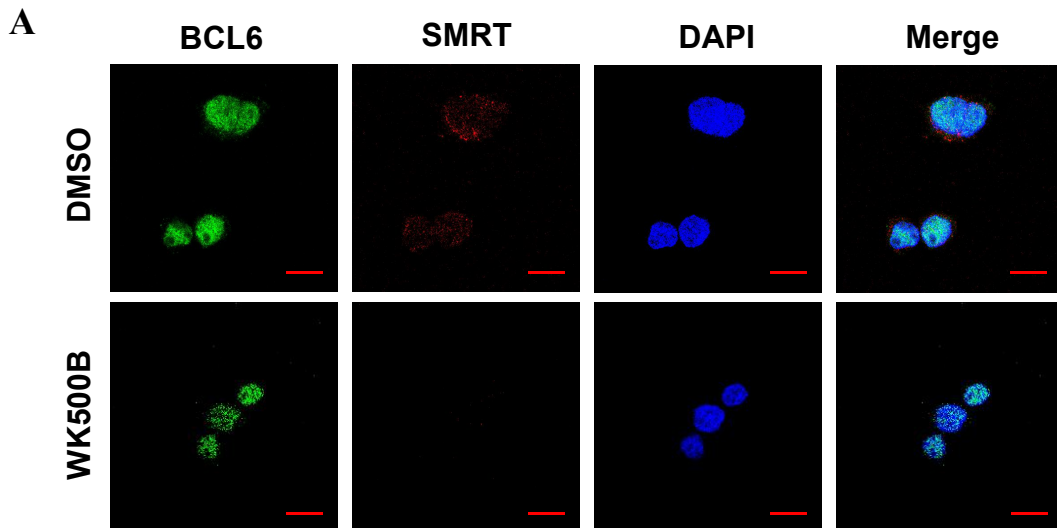


E

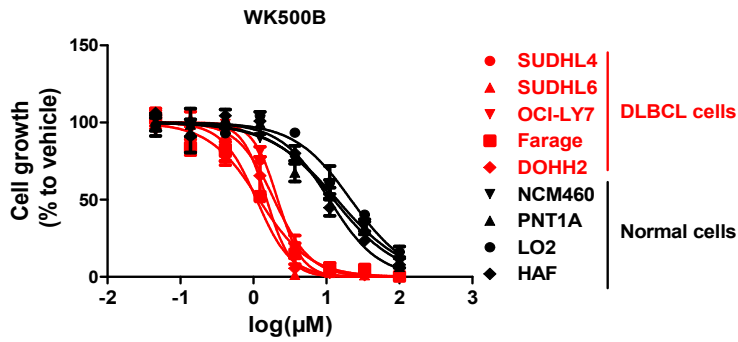


F





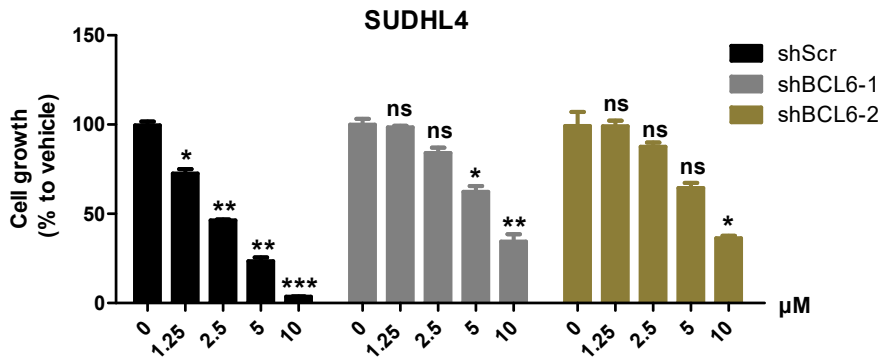
A



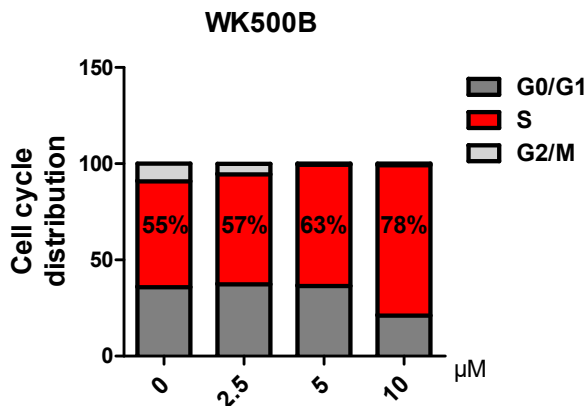
B

	Cell lines	Compounds	
		WK500B	FX1
		IC ₅₀ (μM)	
DLBCL Cells	SUDHL4	1.93 \pm 0.28	67.24 \pm 1.83
	SUDHL6	1.10 \pm 0.43	23.87 \pm 2.65
	OCI-LY7	2.16 \pm 0.33	63.01 \pm 1.79
	Farage	1.19 \pm 0.77	64.37 \pm 6.25
	DOHH2	1.52 \pm 0.18	18.90 \pm 1.28
Normal cells	NCM460	13.99 \pm 2.11	>100
	PNT1A	12.61 \pm 0.22	>100
	LO2	21.61 \pm 2.81	>100
	HAF	11.02 \pm 1.37	>100

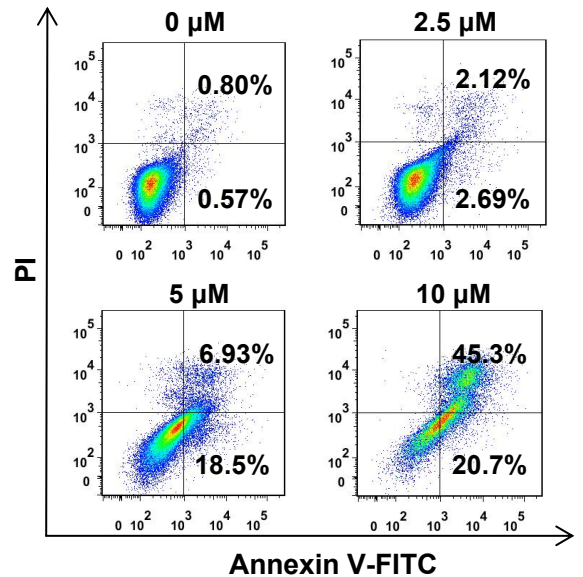
C

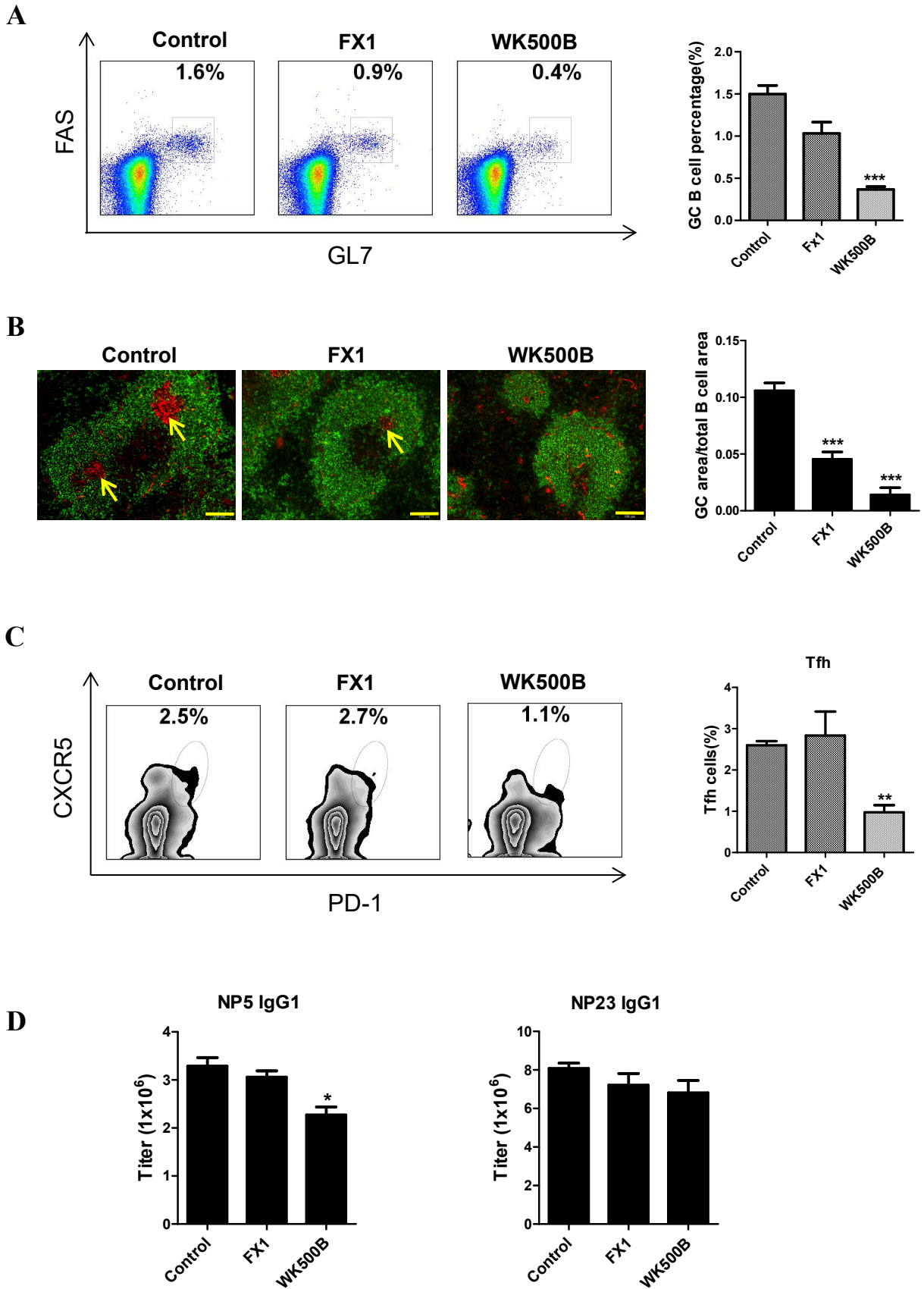


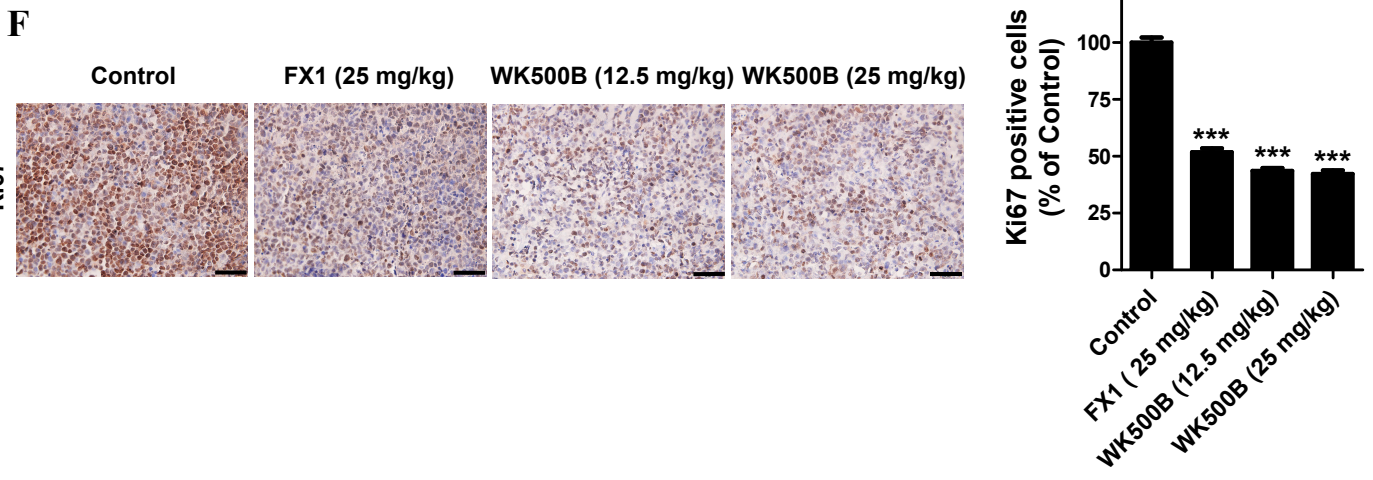
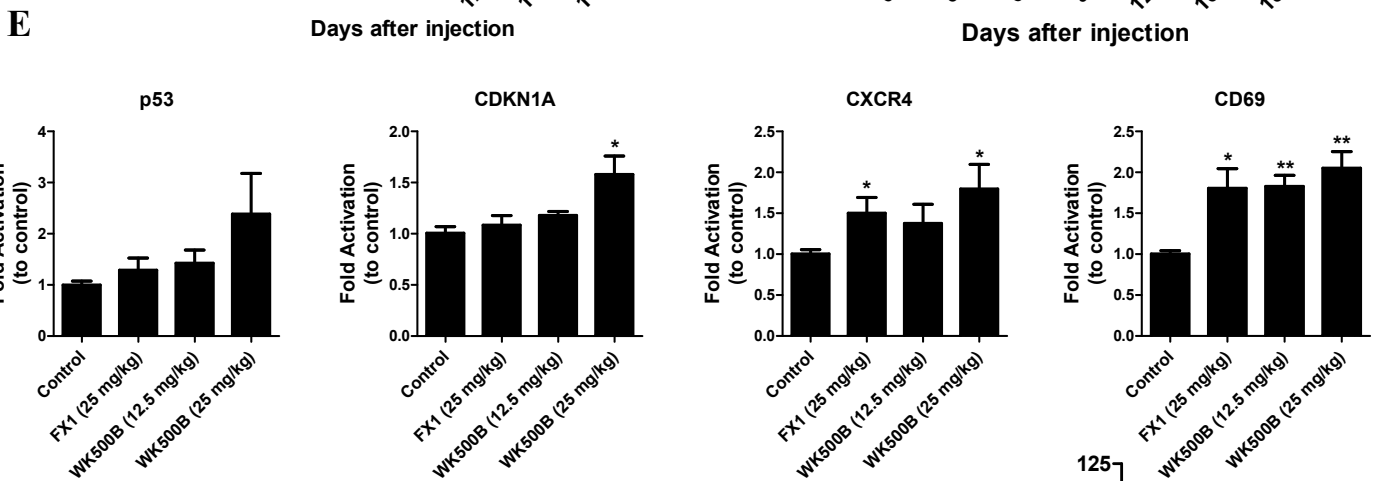
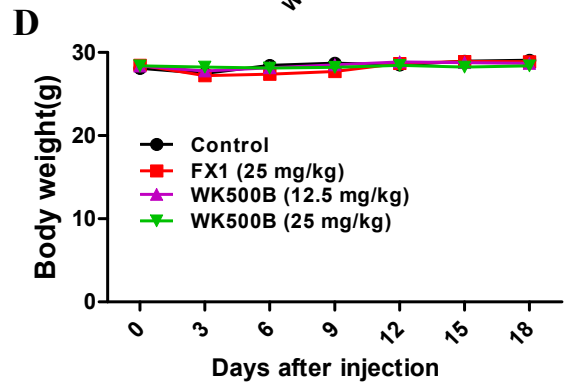
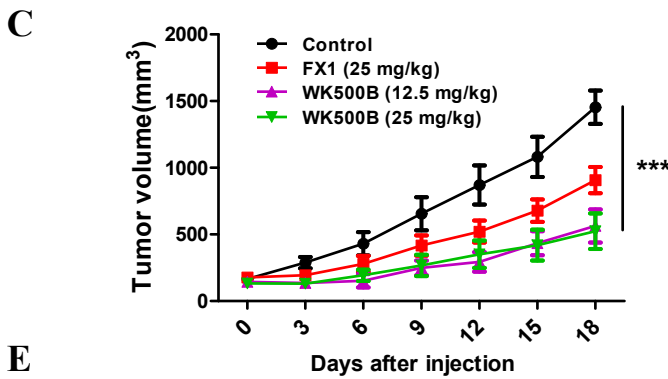
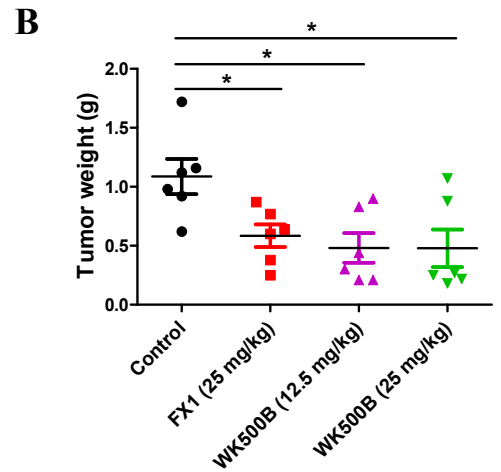
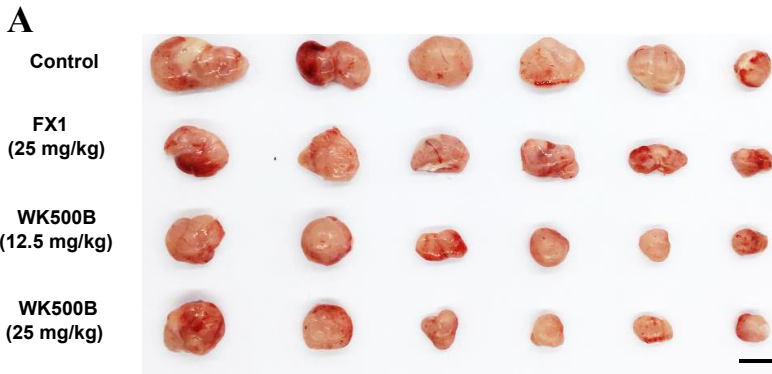
D



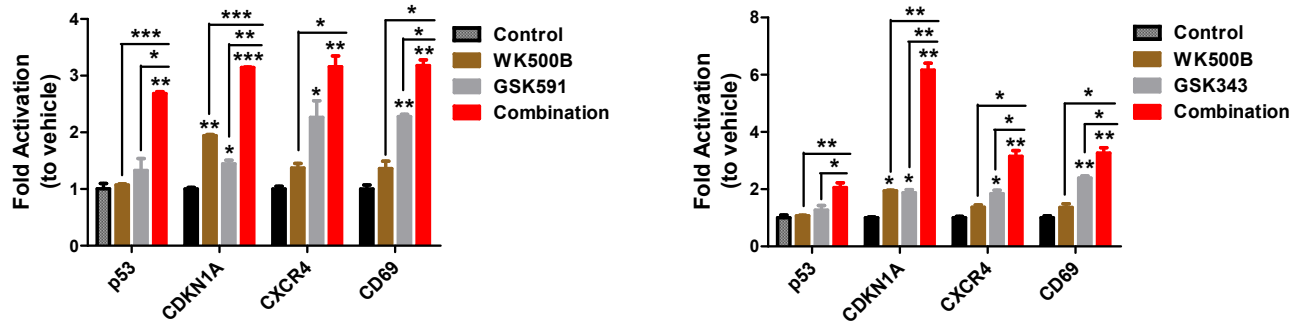
E



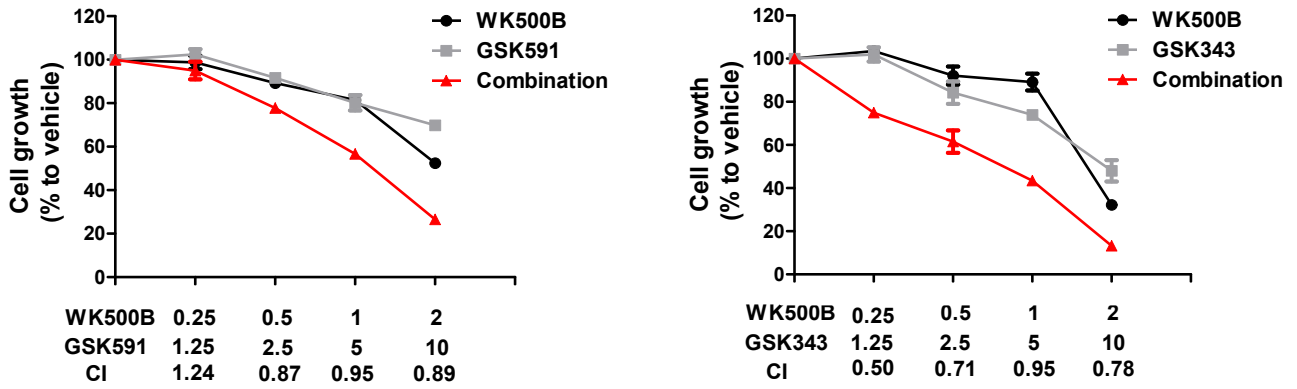




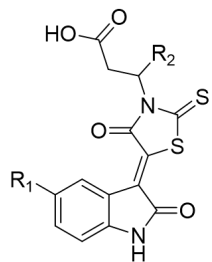
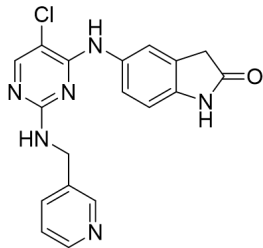
A



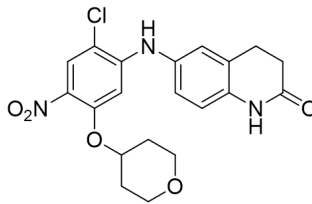
B



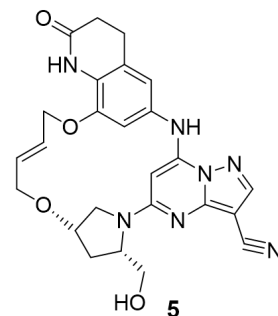
A

1 (79-6): R₁ = Br, R₂ = COOH2 (FX1): R₁ = Cl, R₂ = H

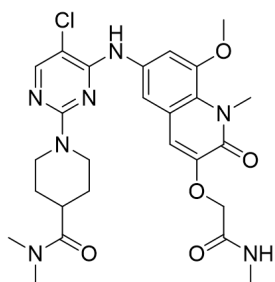
3



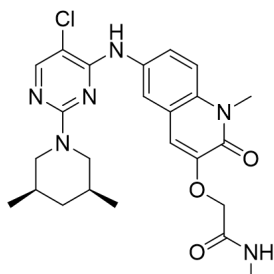
4



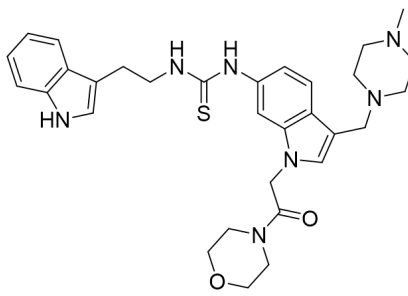
5



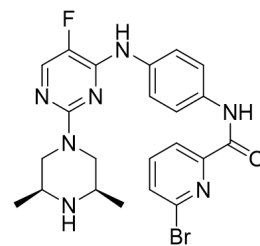
6 (BI3812)



7 (BI3802)



8



WK500B

B

BCL6 inhibitor	Lipinski's rule of five			Reactive BCL6 target genes	Inhibition BCL6 biology function in vivo study	orally available for in vivo study
	MW <500	CLogP < 5	tPSA < 140-90			
WK500B	500.38	Y	Y	Y	Y	Y
1(79-6)	Y	Y	Y	Y	Y	N
2(FX1)	Y	Y	86.71	Y	Y	N
3	Y	Y	Y	Y	N	N
4	Y	Y	Y	N	N	N
5	Y	Y	Y	N	N	N
6(BI3812)	N	Y	Y	N	N	N
7(BI3802)	Y	Y	Y	Y	N	N
8	573.76	Y	75.35	N	N	N